BIBECHANA
Vol. 20, No. 3, December 2023, 309-315

ISSN 2091-0762 (Print), 2382-5340 (Online)
Journal homepage: http://nepjol.info/index.php/BIBECHANA
Publisher: Dept. of Phys., Mahendra Morang A. M. Campus (Tribhuvan University) Biratnagar

Exploring topological phase transition in $Pt_2Hg_{1-x}Tl_xSe_3$

Deergh Bahadur Shahi, Dipak Bhattarai, Madhav Prasad Ghimire*

[1]*Central Department of Physics, Tribhuvan University, Kirtipur, 44613,Kathmandu, Nepal*

*Corresponding author. Email: madhav.ghimire@cdp.tu.edu.np

Abstract

The transition from trivial to non-trivial phase in two-dimensional materials are called a topological phase transition (TPT). The Berry phase, non-local string order parameter, and edge states define the topological nature of the system. A newly discovered jacutingaite material Pt_2HgSe_3 is a layered material which occurs naturally in the form of minerals. The material can be exfoliated and was predicted as a quantum spin Hall insulator. Here, on the basis of density functional theory and tight-binding calculations, we explore $Pt_2Hg_{1-x}Tl_xSe_3$ (x = 0.25, 0.50, 0.75, 1) to understand the electronic and topological properties. We start with the parent material Pt_2HgSe_3 wherein Hg is replaced partially with x amount of Tl, to tune the topological phases. From the electronic structure calculations, Pt_2HgSe_3 is found to be a non-trivial semimetal in it's bulk. Upon electron doping, the material transforms to strong topological metallic phase. The topological Z_2 invariant calculation shows TPT in $Pt_2Hg_{1-x}Tl_xSe_3$ with weak topological insulating state (0;001) for x=0, to strong topological metal (1;000) for x=1, respectively.

Keywords

Density functional theory, Jacutingaite materials, Spin-orbit coupling, Topological invariants, Topological phase transition.

Article information

Manuscript received: September 16, 2023; Accepted: November 1, 2023
DOI https://doi.org/10.3126/bibechana.v20i3.58632

1 Introduction

Topological concept in material science has a crucial role in condensed matter and materials science. Topological notion not only enhances the understanding of various physical phenomena, but also play an important role in the development and innovation in materials science [1]. The study of topological properties is thriving research area due to its promising applications in electronics and quantum computing. Topology and topological invariants plays a significant role in understanding and classification of new states of matter in material science. By using the concepts of mirror Chern number, chern number and topological invariant (Z_2) we can explain the properties and different behaviors exhibited by various quantum Hall systems, topological insulators (TIs), topological semimetals

such as Dirac, Weyl and nodal line.

The surface or edge effects in topological materials are found to change in several properties such as in electronic, optical, transport, magnetic, etc. [2,3] and can be detected using transmission electron microscopy. Two-dimensional (2D) quantum spin Hall insulator (QSHI) are characterized by a gapless helical edge states with small electronic band gap in it's bulk. Though they resists interaction and disorder extending up to room temperature, the study related to QSHI are limited [4,5]. Topological features of the materials can be identified by calculating the Z_2 invariant. Z_2 consists of four components: ν_0; ν_1, ν_2, ν_3 based on which the material can be distinguished whether they are strong or weak topological materials. For instance, when $\nu_0 = 1$; and any of its ν_1, ν_2, ν_3 are either 0 or 1, the material are called strong topological insulator/metal, but, if $\nu_0 = 0$ and any other invariants (ν_1, ν_2, ν_3) are non-zero, they are called weak topological material.

Among several group of materials, Pt_2HgSe_3 is one of the natural mineral of platinum group belonging to jacutingaite family discovered in 2008 [6] and successfully synthesized in 2012 [7–10]. This material has been cleaved to its monolayer and from the density functional theory (many-body G_0W_0 calculations, it was reported to be a QSHI with a band gap of ∼0.15 eV (0.5 eV) at the Dirac point [11]. QSHI to quantum anamolous Hall (QAH) phase was also observed in monolayer of Pt_2HgSe_3 by chemical functionalization [12].

In materials belonging to topological materials, topological phase transition (TPT) can be achieved by chemical functionalization, applying magnetic and electric field, pressure and doping, etc. TPT has been observed in bilayer of jacutingaite when perpendicular electric field was applied wherein the bilayer changes from a normal insulator to QSHI [13]. Likewise, unconventional superconductivity was observed in monolayer of Pt_2HgSe_3 by electron and hole doping along with other exotic property such as QSHI [14]. Monolayer of Pt_2HgSe_3 has also been studied recently in which the material losses its symmetric behavior due to presence of ferromagnetic substrate ($NiBr_2$). Charge transfer takes place at the interface resulting in spin degeneracy band gap of ∼134.2 meV and valley dependent global gap of 58.8 meV, respectively [15]. Further, it was noticed that lattice defect can shift the Fermi level (E_F) above the van Hove singularity in Pt_2HgSe_3 , and thus can potentially serve as an effective means to regulate doping effect [16].

Band inversion is one of the key parameter that dictates the nontrivial property and is associated with a bulk topological invariant. Further, calculation of parities in the Brillouin zone (BZ) of occupied bands at the time reversal invariant momentum (TRIM) are used in determining the topological invariant of the system following inversion symmetry [17]. Thus, in inversion symmetric system, a material with strong spin-orbit coupling (SOC) strength is required to flip the maximum of the valence band to the minimum of conduction band with opposite parities at the TRIM point. This allows to change the phase from normal insulator (NI) to topological insulator (TI). In topological band inversion, band gap is denoted by a negative sign to distinguish it from a trivial band gap in an even topological invariant scenario. TI to NI phase transition was observed also by nonmagnetic substitution [18–20]. While the overall idea of such a transition seems intuitive, specifics are yet unknown. Therefore we can expect that the band gap of a TI would decrease linearly on substitution of a lighter element with weaker SOC strength. The traditional interpretation of nonmagnetic doping phase transition behavior in TIs has been challenged by the low concentration (x), say about 5% in $(Bi_{1-x}In_x)_2Se_3$ system. The low concentration of x in a linear band-closure system, has been carried out by several experimental groups [20, 21].

Essentially, a good dopant should have a shallow defect level and reach optimal solubility in its host material, however, performance of the device is significantly impacted by a few basic doping constraints. For instance, it was discovered that n-type and p- type doping in ZnO were challenging [22]. Consequently, bipolar doping issues arise in numerous large band gap semiconductors, wherein dopants of either the n-type or p-type semiconductor can be introduced, rather than both [23]. Therefore, materials' qualities such as carrier density, mechanical strength, and magnetism are found to change through doping or alloying method [24]. Here, by means of electron doping to Hg site in Pt_2HgSe_3 we report that with increase in doping concentration the material undergoes topological phase transition.

2 Crystal Structure and Computational Details

The crystal structure of Pt_2HgSe_3 is shown in Figure 1 and belongs to space group P-3m1 (space group number 164). The crystal consist of 12 atoms in a unit cell with two structural formula unit (Z = 2). Unit cell of Pt_2HgSe_3 jacutingaite has two distinct position of platinum denoted as Pt1 and Pt2. Six selenium atoms encircle Pt1, while the Pt2 are connected to Hg atoms positioned at the middle of a planar square of selenium atoms (see Fig. 1).

The lattice parameters of Pt_2HgSe_3 used for our calculations are a = 7.3477 Å and c = 5.2955 Å with lattice angles $\alpha = 90^0$, $\beta = 90^0$ and $\gamma = 120^0$. The corresponding atomic positions are [0, 0, 0] for Pt1, [-1/2, 0, 0] for Pt2, [1/3, -1/3, 0.3507] for Hg and

[-0.1804, 0.1804, 0.2492] for Se, respectively.

We perform the density functional theory (DFT) calculations both in the scalar and full-relativistic mode using the full-potential local orbital code (FPLO) version 22.00-62 [25]. Doping effects has been considered in $Pt_2Hg_{1-x}Tl_xSe_3$ (x = 0.25, 0.50,0.75 and 1) by means of virtual crystal approximation (VCA) method implemented in the FPLO code. The standard generalized-gradient approximation (GGA) in the parametrization of Perdew, Burke, and Ernzerhof (PBE) [26] has been used for the exchange-correlation potential. A 16×16×16 k-mesh grid was used in the irreducible BZ for the self-consistent calculations. The energy and charge convergence criteria are set to 10^{-8} Hartree and 10^{-6} C, respectively.

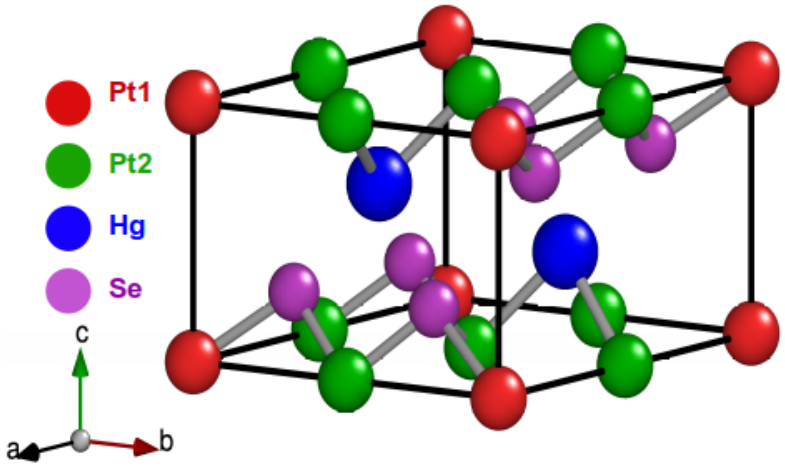

Figure 1: Crystal structure of jacutingaite Pt_2HgSe_3 having hexagonal crystal system.

3 Results and Discussion

Electronic Structure: Here we show the results for the parent material Pt_2HgSe_3 and the end material Pt_2TlSe_3. From the total and partial density of states (DOS) shown in Figure 2a for Pt_2HgSe_3, it can be observed that the major contribution are from Se-4p orbitals hybridizing with the inequivalent Pt-5d, and Hg-6s orbitals extending in the valence region from -1 eV upto the conduction region, with a crossover at E_F. Band structure for the parent material Pt_2HgSe_3 is shown in Fig. 2b within scalar and full-relativistic (with SOC) mode. Without SOC, the two Dirac crossing were observed at K and H close to E_F. With the application of SOC, Dirac points at high symmetry points are gapped with a band gap of ∼30.3 meV at point H as shown in Fig. 2b (inset) followed by band inversion revealing the topological semimetallic behavior. Moving on to the electronic structure of the end material Pt_2TlSe_3 which results from an electron doping via VCA, the total and partial DOS in the valence and conduction region are found to change abruptly. As seen in Fig. 2c, total DOS at E_F is found to increase significantly giving rise to metallic state. The main reason for accumulation of large DOS at E_F is due to the electron occupancy. The total DOS in Pt_2TlSe_3 is mainly contributed by Se-4p with substantial contribution from Pt-5d and Tl-6s orbitals.

The orbital-resolved electronic band structure of Pt_2TlSe_3 shows that the major contribution at and around E_F are from Se- $4p_{x,y,z}$, Pt-$5d_{yz}$ and Tl-6s states. Furthermore, it is interesting to note that electron and hole pocket increases along the Γ - A - L – H path in the BZ with increase in Tl doping (see Fig. 2 (b,d)).

Topological Properties: We extend our study to understand the topological properties in jacutingaite materials. As is well-known, four independent topological invariants, (i.e., $Z_2 = \nu_0$; $\nu_1\ \nu_2\ \nu_3$) proposed by Fu and Kane [27] is given by

$$(-1)_0^{\nu} = \prod_{n_i=0,1} \delta n1 \delta n2 \delta n3 \qquad (1)$$

$$(-1)_0^{\nu} = \prod_{n_j \neq i=0,1; n_i=1} \delta n1 \delta n2 \delta n3 \qquad (2)$$

Connecting it with the bulk band structures of Pt_2HgSe_3 and Pt_2TlSe_3 (see Fig. 2 (b, d), it reveals that at each k-point the conduction band and the valence band are gapped. This allows us to define Z_2 index [28]. Basing on this, we perfrom Z_2 invariant calculations. Note that, for 3D systems, odd Z_2 ($\nu_0 = 1$) index signify strong TI, whereas for even Z_2 ($0 = 0$) index with odd indices for the other three ($\nu_1\ \nu_2\ \nu_3$) characterizes the signature of weak TIs. Thus Z_2 index indicates the distribution of gapless surface states at TRIM in the BZ of 2D surface. Two fold degenerate four occupied bands between energy range -1 to 0.8 eV are used to calculate the

Z_2 invariants by using FPLO code [25]. Our calculation shows that Z_2 index is [0;001] for Pt_2HgSe_3 and [1;000] for Pt_2TlSe_3. This clearly suggest that the parent material Pt_2TlSe_3 is a weak TI while the end material Pt_2TlSe_3 is a strong TI. Z_2 invariants for different values of x concentration in $Pt_2Hg_{1-x}Tl_xSe_3$ are also summarized in Table 1.

In a crystal lattice with inversion symmetric system, Wannier charge center (WCC) are used to calculate Z_2 index. Yu and co-workers recently predicted the topological transition in Sb_2Mg_3 by calculating the Z_2 invariant which was based on U(2N) non-Abelian Berry connection [29,30]. For this, the number of crossing to any horizontal reference line and evolution of WCC in k-space in a random direction are used to calculate the topological invariant. With odd number of crossings to a reference gives rise to $Z_2 = 1$, confirming the topological phase of system. Likewise, an even number of crossing to the reference line will characterize $Z_2 = 0$, indicating a trivial phase of system. Following this we computed the WCC.

From our calculations of Z_2 for the highest occupied molecular orbital, represented by band number 88 for Pt_2HgSe_3, and band number 82 for Pt_2TlSe_3, we observed a horizontal reference line (blue line) that intersects the WCC (see Fig. 3). It is interesting to note that the intersection are odd numbers (say one crossing for Pt_2Hge_3 and three crossings for Pt_2HgSe_3 which confirms that the two jacutingaite are topological materials.

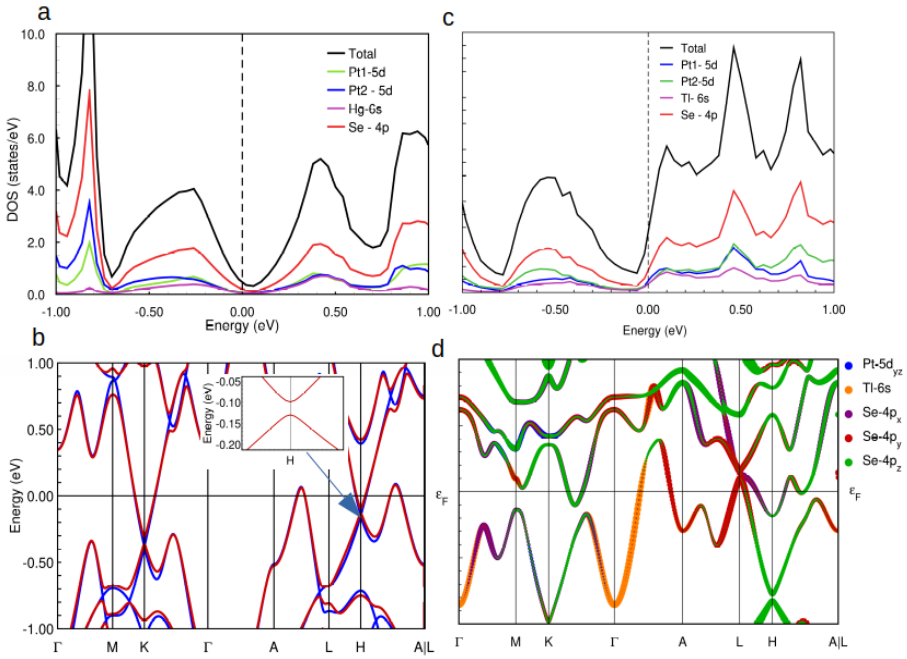

Figure 2: Density of states (a,c) and band structures (b,d) of Pt2HgSe$_3$ (left) and Pt_2TlSe_3 (right). Blue and red colors in Fig. b represents scalar-relativistic and full-relativistic for Pt_2HgSe_3.

Table 1: Calculation of Z_2 invariants.

Z_2 invariants of different material	
Material	$\nu_0;\nu_1\nu_2\nu_3$
Pt_2HgSe_3	0;001
$Pt_2Hg_{0.25}Tl_{0.75}Se_3$	0;001
$Pt_2Hg_{0.5}Tl_{0.5}Se_3$	0;001
$Pt_2Hg_{0.75}Tl_{0.25}Se_3$	0;001
Pt_2TlSe_3	1;000

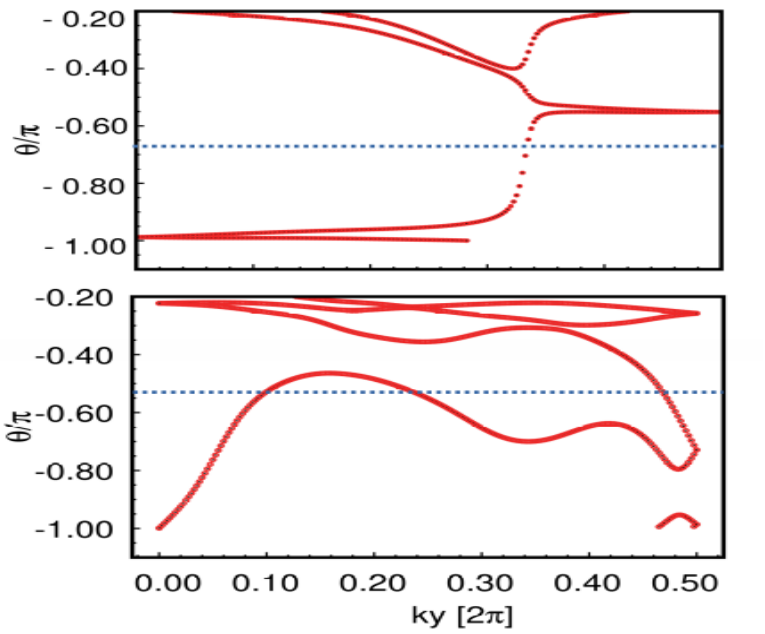

Figure 3: Wannier centers and reference line for band 88 of Pt_2HgSe_3 (top) and band 82 of Pt_2TlSe_3 (bottom).

4 Conclusion

We studied the electronic and topological properties of $Pt_2Hg_{1-x}Tl_xSe_3$ by means of density functional theory and tight-binding calculations using FPLO code [25]. Topological invariants Z_2 are computed by taking Wannier function as a Bloch function. Pt_2HgSe_3 is found to be a weak topological semimetal while Pt_2TlSe_3 is predicted as a strong topological metal. This is confirmed by the odd number of intersection from the Wannier charge center. Thus a topological phase transitions are noted in $Pt_2Hg_{1-x}Tl_xSe_3$ with weak topological insulating state (0;001) for x=0, to strong topological metal (1;000) for x=1, respectively.

Acknowledgments

This work was supported by a grant from UNESCO-TWAS and the Swedish International Development Cooperation Agency (SIDA) with TWAS Research Grant Award No. 21-377 RG/PHYS/ASG-FR3240319525. The views expressed herein do not necessarily represent those of UNESCO-TWAS, SIDA or its Board of Governors. D.B. thanks Nepal Academy of Science and Technology for the PhD fellowship. We are thankful to IFW Dresden, Germany for providing large scale computation facility.

Conflict of Interest

The authors claims that there is no conflict of interest.

References

[1] S. Gupta and A. Saxena. The role of topology in materials. *Materials*, 189, 2018. https://doi.org/10.1007/978-3-319-76596-9

[2] B. Yan and S.C. Zhang. Topological materials: Reports on Progress in Physics. 75(9):096501, 2012. https://doi:10.1088/0034-4885/75/9/096501

[3] L. Nguyen, H.-P. Komsa, E. Khestanova, R. J. Kashtiban, J. J. Peters, S. Lawlor, A. M. Sanchez, J. Sloan, R. V. Gorbachev, and I. V. Grigorieva. Atomic defects and doping of monolayer $NbSe_2$. *ACS Nano*, 11(3):2894, 2017. https://doi.org/10.1021/acsnano.6b08036

[4] J. Wang and S. C. Zhang. Topological states of condensed matter. *Nature Materials*, 16(11):1062–1067, 2017. https://doi.org/10.1038/nmat5012

[5] F. Reis, G. Li, L. Dudy, M. Bauernfeind, S. Glass, W. Hanke, R. Thomale, J. Schäfer, and R. Claessen. Bismuthene on a sic substrate: A candidate for a high-temperature quantum spin hall material. *Sci-*

ence, 357(6348):287–290, 2017. https://doi.org/10.1126/science.aai8142

[6] A. Cabral, H. Galbiatti, R. Kwitko-Ribeiro, and B. Lehmann. Terra nova. 20(1):32–37, 2008. https://doi.org/10.1111/j.1365-3121.2007.00783.x

[7] K. Kandrai, P. Vancsó, G. Kukucska, J. Koltai, G. Baranka, Á. Hoffmann, Á. Pekker, K. Kamarás, Z. E. Horváth, and A. Vymazalová. Signature of large-gap quantum spin hall state in the layered mineral jacutingaite. *Nano Letters*, 20(7):5207–5213, 2020. https://doi.org/10.1021/acs.nanolett.0c01499

[8] I. Cucchi, A. Marrazzo, E. Cappelli, S. Riccò, F. Bruno, S. Lisi, M. Hoesch, T. Kim, C. Cacho, and C. Besnard. Bulk and surface electronic structure of the dual-topology semimetal Pt_2HgSe_3. *Phys. Rev. Lett.*, 124(10):106402, 2020. https://doi.org/10.1103/PhysRevLett.124.106402

[9] A. Vymazalová, F. Laufek, M. Drábek, A. R. Cabral, J. Haloda, T. Sidorinová, B. Lehmann, H. F. Galbiatti, and J. Drahokoupil. Jacutingaite, Pt_2HgSe_3, a new platinum-group mineral species from the cauê iron-ore deposit, itabira district, minas gerais, brazil. *The Canadian Mineralogist*, 50(2):431–440, 2012. https://doi.org/10.3749/canmin.50.2.431

[10] R. Longuinhos, A. Vymazalová, A. R. Cabral, S. S. Alexandre, R. W. Nunes, and J. Ribeiro-Soares. Raman spectrum of layered jacutingaite (Pt_2HgSe_3) crystals-experimental and theoretical study. *Journal of Raman Spectroscopy*, 51(2):357–365, 2020. https://doi.org/10.1002/jrs.5764

[11] A. Bafekry, M. Obeid, C. V. Nguyen, M. Ghergherehchi, and M. B. Tagani. Graphene hetero-multilayer on layered platinum mineral jacutingaite (Pt_2HgSe_3), van der waals heterostructures with novel optoelectronic and thermoelectric performances. *Journal of Materials Chemistry A*, 8(26):13248–13260, 2020. https://doi.org/10.1039/D0TA02847A

[12] F. Luo, X. Hao, Y. Jia, J. Yao, Q. Meng, S. Zhai, J. Wu, W. Dou, and M. Zhou. Functionalization induced quantum spin hall to quantum anomalous hall phase transition in monolayer jacutingaite. *Nanoscale*, 13(4):2527–2533, 2021. https://doi.org/10.1039/D0NR06889F

[13] L. Rademaker and M. Gibertini. Gate-tunable imbalanced kane-mele model in encapsulated bilayer jacutingaite. *Phys. Rev. M*, 5(4):044201, 2021. https://doi.org/10.1103/PhysRevMaterials.5.044201

[14] X. Wu, M. Fink, W. Hanke, R. Thomale, and D. Di Sante. Unconventional superconductivity in a doped quantum spin hall insulator. *Physical Review B*, 100(4):041117, 2019. https://doi.org/10.1103/PhysRevB.100.041117

[15] X. Zhu, Y. Chen, Z. Liu, Y. Han, and Z. Qiao. Valley-polarized quantum anomalous hall effect in van der waals heterostructures based on monolayer jacutingaite family materials. *Frontiers of Physics*, 18(2):23302, 2023. https://doi.org/10.48550/arXiv.2211.14109

[16] K. Kandrai, P. Vancsó, G. Kukucska, J. Koltai, G. Baranka, Á. Hoffmann, and P. Nemes-Incze. Signature of large-gap quantum spin hall state in the layered mineral jacutingaite. *Nano Letters*, 20(7):5207–5213, 2020. https://doi.org/10.1021/acs.nanolett.0c01499

[17] L. Fu and C. L. Kane. Topological insulators in three dimensions. *Phys. Rev. Lett.*, 98(10):106803, 2007. https://doi.org/10.1103/PhysRevLett.98.106803

[18] T. Sato, K. Segawa, K. Kosaka, S. Souma, K. Nakayama, K. Eto, T. Minami, Y. Ando, and T. Takahashi. Unexpected mass acquisition of dirac fermions at the quantum phase transition of a topological insulator. *Nature Physics*, 7(11):840–844, 2011. https://doi.org/10.1038/nphys2058

[19] S.-Y. Xu, Y. Xia, L. Wray, S. Jia, F. Meier, J. Dil, J. Osterwalder, B. Slomski, A. Bansil, and H. Lin. Topological phase transition and texture inversion in a tunable topological insulator. *Science*, 332(6029):560–564, 2011. https://doi.org/10.1126/science.1201607

[20] S. Chadov, J. Kiss, C. Felser, K. Chadova, D. Ködderitzsch, J. Minár, and H. Ebert. Topological phase transition induced by random substitution. *arXiv preprint arXiv:1207*, page 3463, 2012. https://doi.org/10.48550/arXiv.1207.346

[21] M. Brahlek, N. Bansal, N. Koirala, S.-Y. Xu, M. Neupane, C. Liu, M. Z. Hasan, and S. Oh. Topological-metal to band-insulator transition in $(Bi_{1-x}In_x)_2Se_3$ thin films. *Phys. Rev. Lett.*, 109(18):186403, 2012. https://doi.org/10.1103/PhysRevLett.109.186403

[22] C. Freysoldt, B. Grabowski, T. Hickel, J. Neugebauer, G. Kresse, A. Janotti, and C. G. Van de Walle. First-principles calculations for point defects in solids. *Reviews of Modern Physics*, 86(1):253, 2014. https://doi.org/10.1103/RevModPhys.86.253

[23] S.-H. Wei. Overcoming the doping bottleneck in semiconductors. *Computational Materials Science*, 30(3-4):337–348, 2004. https://doi.org/10.1016/j.commatsci.2004.02.024

[24] S. Pearton, C. Abernathy, M. Overberg, G. Thaler, D. Norton, N. Theodoropoulou, A. Hebard, Y. Park, F. Ren, and J. Kim. Wide band gap ferromagnetic semiconductors and oxides. *Journal of Applied Physics*, 93(1):1–13, 2003. https://doi.org/10.1063/1.1517164

[25] K. Koepernik and H. Eschrig. Full-potential nonorthogonal local-orbital minimum-basis band-structure scheme. *Phys. Rev. B*, 59(3):1743, 1999. https://doi.org/10.1103/PhysRevB.59.1743

[26] J. P. Perdew, K. Burke, and M. Ernzerhof. Generalized gradient approximation made simple. *Phys. Rev. Lett.*, 77(18):3865, 1996. https://doi.org/10.1103/PhysRevLett.77.3865

[27] J. I. Facio, S. K. Das, Y. Zhang, K. Koepernik, J. van den Brink, and I. C. Fulga. Dual topology in jacutingaite Pt_2HgSe_3. *Phys. Rev. M*, 3(7):074202, 2019. https://doi.org/10.1103/PhysRevMaterials.3.074202

[28] U. Dey, M. Chakraborty, A. Taraphder, and S. Tewari. Bulk band inversion and surface dirac cones in LaSb and LaBi: Prediction of a new topological heterostructure. *Scientific Reports*, 8(1):14867, 2018. https://doi.org/10.1038/s41598-018-33273-6

[29] R. Yu, X. L. Qi, A. Bernevig, Z. Fang, and X. Dai. Equivalent expression of Z_2 topological invariant for band insulators using the non-abelian berry connection. *Phys. Rev. B*, 84(7):075119, 2011. https://doi.org/10.1103/PhysRevB.84.075119

[30] Y. Sun, X.-Q. Chen, S. Yunoki, D. Li, and Y. Li. New family of three-dimensional topological insulators with antiperovskite structure. *Phys. Rev. Lett.*, 105(21):216406, 2010. https://doi.org/10.1103/PhysRevLett.105.216406